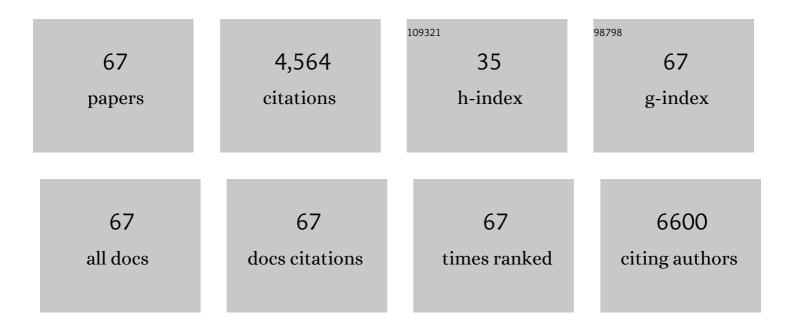
## Seung Min Kim

List of Publications by Year in descending order

Source: https://exaly.com/author-pdf/11397429/publications.pdf Version: 2024-02-01



#	Article	IF	CITATIONS
1	Preferential Growth of Single-Walled Carbon Nanotubes with Metallic Conductivity. Science, 2009, 326, 116-120.	12.6	397
2	Size and Support Effects for the Water–Gas Shift Catalysis over Gold Nanoparticles Supported on Model Al <sub>2</sub> O <sub>3</sub> and TiO <sub>2</sub> . Journal of the American Chemical Society, 2012, 134, 4700-4708.	13.7	380
3	Role of Water in Super Growth of Single-Walled Carbon Nanotube Carpets. Nano Letters, 2009, 9, 44-49.	9.1	371
4	Investigation of Changes in the Surface Structure of Li <sub><i>x</i></sub> Ni <sub>0.8</sub> Co <sub>0.15</sub> Al <sub>0.05</sub> O <sub>2</sub> Cathode Materials Induced by the Initial Charge. Chemistry of Materials, 2014, 26, 1084-1092.	6.7	308
5	Influence of Alumina Type on the Evolution and Activity of Alumina-Supported Fe Catalysts in Single-Walled Carbon Nanotube Carpet Growth. ACS Nano, 2010, 4, 895-904.	14.6	201
6	Evolution in Catalyst Morphology Leads to Carbon Nanotube Growth Termination. Journal of Physical Chemistry Letters, 2010, 1, 918-922.	4.6	177
7	Metallic Corner Atoms in Gold Clusters Supported on Rutile Are the Dominant Active Site during Waterâ^'Gas Shift Catalysis. Journal of the American Chemical Society, 2010, 132, 14018-14020.	13.7	170
8	Highly Crystalline CVD-grown Multilayer MoSe2 Thin Film Transistor for Fast Photodetector. Scientific Reports, 2015, 5, 15313.	3.3	129
9	Direct spinning and densification method for high-performance carbon nanotube fibers. Nature Communications, 2019, 10, 2962.	12.8	126
10	Genesis and Evolution of Surface Species during Pt Atomic Layer Deposition on Oxide Supports Characterized by in Situ XAFS Analysis and Waterâ^'Gas Shift Reaction. Journal of Physical Chemistry C, 2010, 114, 9758-9771.	3.1	124
11	Double-Walled Boron Nitride Nanotubes Grown by Floating Catalyst Chemical Vapor Deposition. Nano Letters, 2008, 8, 3298-3302.	9.1	109
12	Highâ€Mobility Transistors Based on Largeâ€Area and Highly Crystalline CVDâ€Grown MoSe <sub>2</sub> Films on Insulating Substrates. Advanced Materials, 2016, 28, 2316-2321.	21.0	107
13	Using Real-Time Electron Microscopy To Explore the Effects of Transition-Metal Composition on the Local Thermal Stability in Charged Li <sub><i>x</i></sub> Ni <sub><i>y</i></sub> Mn <sub><i>z</i></sub> Co <sub>1–<i>y</i>–<i>z</i></sub> C Cathode Materials, Chemistry of Materials, 2015, 27, 3927-3935.	D<\$ub>2 </td <td>103 sub&gt;</td>	103 sub>
14	A highly sensitive chemical gas detecting transistor based on highly crystalline CVD-grown MoSe2 films. Nano Research, 2017, 10, 1861-1871.	10.4	102
15	Direct one-pot conversion of monosaccharides into high-yield 2,5-dimethylfuran over a multifunctional Pd/Zr-based metal–organic framework@sulfonated graphene oxide catalyst. Green Chemistry, 2017, 19, 2482-2490.	9.0	97
16	Investigating Local Degradation and Thermal Stability of Charged Nickel-Based Cathode Materials through Real-Time Electron Microscopy. ACS Applied Materials & Interfaces, 2014, 6, 15140-15147.	8.0	90
17	A route to synthesis molybdenum disulfide-reduced graphene oxide (MoS2-RGO) composites using supercritical methanol and their enhanced electrochemical performance for Li-ion batteries. Journal of Power Sources, 2016, 309, 202-211.	7.8	89
18	High-modulus and strength carbon nanotube fibers using molecular cross-linking. Carbon, 2017, 118, 413-421.	10.3	83

#	Article	IF	CITATIONS
19	Investigating the Reversibility of Structural Modifications of Li <sub><i>x</i></sub> Ni <sub><i>y</i></sub> Mn <sub><i>z</i></sub> Co <sub>1–<i>y</i>–<i>z</i></sub> O< Cathode Materials during Initial Charge/Discharge, at Multiple Length Scales. Chemistry of Materials, 2015, 27, 6044-6052.	(sub>2 <td>ubs</td>	ubs
20	Highly-efficient and magnetically-separable ZnO/Co@N-CNTs catalyst for hydrodeoxygenation of lignin and its derived species under mild conditions. Green Chemistry, 2019, 21, 1021-1042.	9.0	72
21	Direct conversion of cellulose to high-yield methyl lactate over Ga-doped Zn/H-nanozeolite Y catalysts in supercritical methanol. Green Chemistry, 2017, 19, 1969-1982.	9.0	62
22	Ga-doped Cu/H-nanozeolite-Y catalyst for selective hydrogenation and hydrodeoxygenation of lignin-derived chemicals. Green Chemistry, 2018, 20, 3253-3270.	9.0	60
23	Improving the Stability of High-Performance Multilayer MoS <sub>2</sub> Field-Effect Transistors. ACS Applied Materials & Interfaces, 2017, 9, 42943-42950.	8.0	59
24	One-pot di- and polysaccharides conversion to highly selective 2,5-dimethylfuran over Cu-Pd/Amino-functionalized Zr-based metal-organic framework (UiO-66(NH2))@SGO tandem catalyst. Applied Catalysis B: Environmental, 2019, 243, 337-354.	20.2	58
25	Hydrogen-Enriched Reduced Graphene Oxide with Enhanced Electrochemical Performance in Lithium Ion Batteries. Chemistry of Materials, 2015, 27, 266-275.	6.7	53
26	Deep-injection floating-catalyst chemical vapor deposition to continuously synthesize carbon nanotubes with high aspect ratio and high crystallinity. Carbon, 2021, 173, 901-909.	10.3	52
27	Investigation of Thermal Stability of P2–Na <sub><i>x</i></sub> CoO <sub>2</sub> Cathode Materials for Sodium Ion Batteries Using Real-Time Electron Microscopy. ACS Applied Materials & Interfaces, 2017, 9, 18883-18888.	8.0	48
28	Interstitial Moâ€Assisted Photovoltaic Effect in Multilayer MoSe <sub>2</sub> Phototransistors. Advanced Materials, 2018, 30, e1705542.	21.0	48
29	Syntheses of Boron Nitride Nanotubes from Borazine and Decaborane Molecular Precursors by Catalytic Chemical Vapor Deposition with a Floating Nickel Catalyst. Chemistry of Materials, 2012, 24, 2872-2879.	6.7	46
30	High-strength carbon nanotube/carbon composite fibers via chemical vapor infiltration. Nanoscale, 2016, 8, 18972-18979.	5.6	46
31	Catalyst and catalyst support morphology evolution in single-walled carbon nanotube supergrowth: Growth deceleration and termination. Journal of Materials Research, 2010, 25, 1875-1885.	2.6	43
32	Effect of oxygen plasma treatment on the mechanical properties of carbon nanotube fibers. Materials Letters, 2015, 156, 17-20.	2.6	42
33	Investigating the Kinetic Effect on Structural Evolution of Li <sub><i>x</i></sub> Ni <sub>0.8</sub> Co <sub>0.15</sub> Al <sub>0.05</sub> O <sub>2</sub> Cathode Materials during the Initial Charge/Discharge. Chemistry of Materials, 2017, 29, 2708-2716.	6.7	39
34	One-pot direct conversion of levulinic acid into high-yield valeric acid over a highly stable bimetallic Nb-Cu/Zr-doped porous silica catalyst. Green Chemistry, 2020, 22, 766-787.	9.0	39
35	Significantly Increased Solubility of Carbon Nanotubes in Superacid by Oxidation and Their Assembly into Highâ€Performance Fibers. Small, 2017, 13, 1701131.	10.0	38
36	Synthesis and lithium storage properties of MoS 2 nanoparticles prepared using supercritical ethanol. Chemical Engineering Journal, 2016, 285, 517-527.	12.7	33

Seung Min Kim

#	Article	IF	CITATIONS
37	Mechanical and electrical properties of thermochemically cross-linked polymer carbon nanotube fibers. Composites Part A: Applied Science and Manufacturing, 2016, 91, 222-228.	7.6	31
38	Rapid and Scalable Reduction of Dense Surface-Supported Metal-Oxide Catalyst with Hydrazine Vapor. ACS Nano, 2009, 3, 1897-1905.	14.6	27
39	Structural Evolution of Li <sub><i>x</i></sub> Ni <sub><i>y</i></sub> Mn <sub><i>z</i></sub> Co <sub>1-y-z</sub> O <sub>2</sub> Cathode Materials during High-Rate Charge and Discharge. Journal of Physical Chemistry Letters, 2017, 8. 5758-5763.	4.6	27
40	Different thermal degradation mechanisms: Role of aluminum in Ni-rich layered cathode materials. Nano Energy, 2020, 78, 105367.	16.0	27
41	A Mechanistic Understanding of Nonclassical Crystal Growth in Hydrothermally Synthesized Sodium Yttrium Fluoride Nanowires. Chemistry of Materials, 2020, 32, 2753-2763.	6.7	27
42	Accurate measurement of specific tensile strength of carbon nanotube fibers with hierarchical structures by vibroscopic method. RSC Advances, 2017, 7, 8575-8580.	3.6	26
43	Mathematical model for the dynamic mechanical behavior of carbon nanotube yarn in analogy with hierarchically structured bio-materials. Carbon, 2019, 152, 151-158.	10.3	25
44	Determination of the mechanism and extent of surface degradation in Ni-based cathode materials after repeated electrochemical cycling. APL Materials, 2016, 4, .	5.1	24
45	Photoacoustic effect on the electrical and mechanical properties of polymer-infiltrated carbon nanotube fiber/graphene oxide composites. Composites Science and Technology, 2017, 153, 136-144.	7.8	21
46	Synthesis, property, and application of carbon nanotube fiber. Journal of the Korean Ceramic Society, 2021, 58, 148-159.	2.3	20
47	Fabrication of sustainable and multifunctional TiO2@carbon nanotube nanocomposite fibers. Applied Surface Science, 2021, 541, 148332.	6.1	19
48	The influence of boundary layer on the growth kinetics of carbon nanotube forests. Carbon, 2015, 93, 217-225.	10.3	18
49	Purification effect of carbon nanotube fibers on their surface modification to develop a high-performance and multifunctional nanocomposite fiber. Carbon, 2021, 173, 376-383.	10.3	17
50	Inâ€Depth TEM Investigation on Structural Inhomogeneity within a Primary Li <sub><i>x</i></sub> Ni <sub>0.835</sub> Co <sub>0.15</sub> Al <sub>0.015</sub> O <sub>2</sub> Particle: Origin of Capacity Decay during Highâ€Rate Discharge. Angewandte Chemie - International Edition, 2020, 59, 2385-2391.	13.8	16
51	Improving mechanical and physical properties of ultra-thick carbon nanotube fiber by fast swelling and stretching process. Carbon, 2021, 172, 733-741.	10.3	16
52	Strong and Highly Conductive Carbon Nanotube Fibers as Conducting Wires for Wearable Electronics. ACS Applied Nano Materials, 2021, 4, 3833-3842.	5.0	16
53	Direct observation of morphological evolution of a catalyst during carbon nanotube forest growth: new insights into growth and growth termination. Nanoscale, 2016, 8, 2055-2062.	5.6	14
54	Simultaneous enhancement of mechanical and electrical properties of carbon nanotube fiber by infiltration and subsequent carbonization of resorcinol-formaldehyde resin. Composites Part B: Engineering, 2019, 163, 431-437.	12.0	14

Seung Min Kim

#	Article	IF	CITATIONS
55	High-crystallinity single-walled carbon nanotube aerogel growth: Understanding the real-time catalytic decomposition reaction through floating catalyst chemical vapor deposition. Chemical Engineering Journal Advances, 2022, 10, 100261.	5.2	14
56	Effects of nitrogen doping from pyrolyzed ionic liquid in carbon nanotube fibers: enhanced mechanical and electrical properties. Nanotechnology, 2015, 26, 075706.	2.6	13
57	Rationally designed catalyst layers toward "immortal―growth of carbon nanotube forests: Fe-ion implanted substrates. Carbon, 2019, 152, 482-488.	10.3	13
58	Bio-inspired incorporation of functionalized graphene oxide into carbon nanotube fibers for their efficient mechanical reinforcement. Composites Science and Technology, 2019, 181, 107680.	7.8	10
59	One-pot, cascade conversion of cellulose to γ-valerolactone over a multifunctional Ru–Cu/zeolite-Y catalyst in supercritical methanol. Applied Catalysis B: Environmental, 2022, 314, 121466.	20.2	10
60	Evolution of implanted Fe ions in SiO2/Si wafer into uniformly sized catalyst particles for carbon nanotube forest growth. Carbon, 2017, 123, 122-128.	10.3	9
61	Effects of a SiO <sub>2</sub> sub-supporting layer on the structure of a Al <sub>2</sub> O <sub>3</sub> supporting layer, formation of Fe catalyst particles, and growth of carbon nanotube forests. RSC Advances, 2016, 6, 68424-68432.	3.6	8
62	Singular Grain Boundaries in Alumina Doped with Silica. Journal of the American Ceramic Society, 2004, 87, 507-509.	3.8	7
63	Investigation of carbon nanotube growth termination mechanism by in-situ transmission electron microscopy approaches. Carbon Letters, 2013, 14, 228-233.	5.9	6
64	Inâ€Depth TEM Investigation on Structural Inhomogeneity within a Primary Li x Ni 0.835 Co 0.15 Al 0.015 O 2 Particle: Origin of Capacity Decay during Highâ€Rate Discharge. Angewandte Chemie, 2020, 132, 2406-2412.	2.0	4
65	Using In-Situ Methods to Characterize Phase Changes in Charged Lithium Nickel Cobalt Aluminum Oxide Cathode Materials. Microscopy and Microanalysis, 2019, 25, 2030-2031.	0.4	2
66	Evolution, Activity, and Lifetime of Alumina-supported Fe Catalyst During Super Growth of Single-walled Carbon Nanotube Carpets: Influence of the Type of Alumina. Materials Research Society Symposia Proceedings, 2010, 1258, 1.	0.1	1
67	Reply to Comment on "A Mechanistic Understanding of Nonclassical Crystal Growth in Hydrothermally Synthesized Sodium Yttrium Fluoride Nanowires― Chemistry of Materials, 2021, 33, 3862-3864.	6.7	1